

Self-Healing Poly(acrylic acid) Hydrogels: Effect of Surfactant

Umit Gulyuz,* Oguz Okay

Summary: Physical poly(acrylic acid) gels were prepared by micellar copolymerization of hydrophilic monomer acrylic acid with large hydrophobic monomer stearyl methacrylate (C18) in solutions of worm-like anionic surfactant (sodium dodecyl sulfate, SDS) and cationic surfactant (cetyltrimethyl ammonium bromide, CTAB) micelles. Hydrophobe content of the monomer mixtures was 2 mol.% and total monomer concentration in gels was 20 w/v%. Gelation reactions were monitored by rheometry using oscillatory deformation tests. Hydrogel samples were also subjected to uniaxial elongation and compression tests after preparation and swelling. The physical gels with SDS and CTAB showed similar properties as long as they are at the state of preparation, such as insoluble in water and exhibit time-dependent dynamic moduli, high Young's modulus, high fracture stress, high elongation ratios at break. Also self-healing was evidenced by mechanical measurements. Physical gels formed in SDS solution were stable, exhibited high equilibrium swelling ratios and SDS progressively extracted from the network in water. On the other hand, gels with CTAB formed a complex and resulted in shrinkage after gels were immersed in a large excess of water because both electrostatic interactions between the charged components and hydrophobic interactions between the polymer backbone and the alkyl chains of the surfactant are important in driving the self-assembly of molecules to form ordered structures. These structures of the polyelectrolyte surfactant complexes have unusual mechanical properties. Also, the hydrogel samples with CTAB self-healed via heating and surfactant treatment of the damaged areas withstand up to 1.05 MPa stresses and rupture at a stretch of 800%.

Keywords: hydrogels; poly(acrylic acid); polyelectrolyte; self-healing; surfactants

Introduction

Self-healing is one of the remarkable properties of biological materials such as skin, bones, and wood.^[1] Inspired by natural healing processes, different reversible molecular interactions have been used recently to generate self-healing hydrogels, including hydrogen bonding,^[2,3] electrostatic interactions,^[4,5] molecular recognition,^[6] metal coordination,^[7] π - π stacking,^[8] dynamic chemical bonds^[9,10] and molecular diffusion.^[11,12] Recently, our research group

presented a simple strategy for the production of self-healing hydrogels via hydrophobic interaction.^[13–16] Incorporation of hydrophobic sequences within the hydrophilic polymer chains via micellar polymerization generates dynamic hydrophobic associations between the hydrophobic domains of polymer chains and surfactant micelles acting as physical cross-links of the resulting hydrogels. These reversible breakable cross-links are responsible for rapid self-healing.

In this study, pH responsive physical gels were prepared by micellar copolymerization of hydrophilic monomer acrylic acid (AAc) with large hydrophobic monomer stearyl methacrylate (C18) in solution of

Department of Chemistry, Istanbul Technical University, 34469, Istanbul, Turkey
E-mail: umitgulyuz@itu.edu.tr

worm-like anionic surfactant^[15] (sodium dodecyl sulfate, SDS) and cationic surfactant^[16] (cetyltrimethyl ammonium bromide, CTAB) micelles. Hydrophobe content of the monomer mixtures was 2 mol.% and total monomer concentration in gels was 20 w/v%. Gelation reactions were monitored by rheometry using oscillatory deformation tests. Hydrogel samples were also subjected to uniaxial elongation and compression after preparation and equilibrium in water. Surfactant effect on the rheological and mechanical properties as well as the self-healing abilities of the hydrogels was investigated. As will be seen below, rheological, mechanical and self-healing behaviors of hydrogels formed in SDS and CTAB solutions are similar as long as they are at the state of preparation. However, when upon immersion in water and after extraction of free surfactant micelles, a completely different behavior is observed between gels.

Experimental Section

Acrylic acid (AAc, Merck) was freed from its inhibitor by passing through an inhibitor removal column purchased from the Aldrich Chemical Co. Commercially available stearyl methacrylate (C18, Aldrich) consists of 65% *n*-octadecyl methacrylate and 35% *n*-hexadecyl methacrylate. Sodium dodecyl sulfate (SDS, Sigma), cetyltrimethyl ammonium bromide (CTAB,

Sigma), ammonium persulfate (APS, Sigma-Aldrich), sodium pyrosulfite ($\text{Na}_2\text{S}_2\text{O}_5$, Fluka), sodium chloride (NaCl, Merck) and sodium bromide (NaBr, Merck) were used as received.

Hydrogel Preparation

As illustrated in Figure 1, micellar copolymerization of AAc with 2 mol.% C18 was conducted at 50 °C in the presence of an APS (3.5 mM)– $\text{Na}_2\text{S}_2\text{O}_5$ (1 mM) redox initiator system in surfactant-salt (SDS–NaCl or CTAB–NaBr) solutions. Surfactant and salt concentrations were set to 10% w/v and 0.25 M, respectively. Addition of salt into the reaction solution leads to micellar growth and hence solubilization of large hydrophobes within the grown worm-like micelles.^[13] Incorporation of hydrophobic sequences within the hydrophilic polymer chains via micellar polymerization generates dynamic hydrophobic associations between the hydrophobic domains of polymer chains and surfactant micelles acting as physical cross-links of the resulting hydrogels.

Swelling Measurements

Hydrogel samples were immersed in a large excess of water for at least 15 days by replacing water every day to extract any soluble species. The mass m of the gel samples was monitored as a function of swelling time by weighing the samples. The relative mass m_{rel} of gels with respect to the after preparation state was calculated as

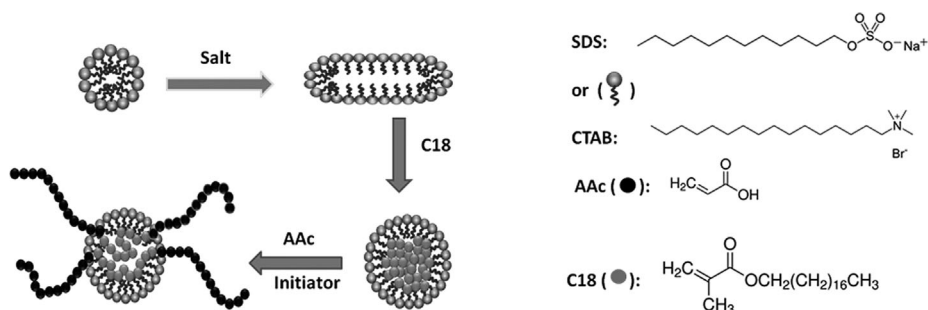


Figure 1.

Cartoon showing the preparation of physical gels in aqueous surfactant-salt solutions via hydrophobic C18 blocks.

$m_{\text{rel}} = m/m_0$, where m_0 is the initial mass of the gel sample.

Mechanical Tests

Uniaxial compression and elongation measurements were performed on cylindrical hydrogel samples after synthesis and after equilibrium in water on a Zwick Roell test machine using 10 and 500 N load cells. Load and displacement data were collected during the experiments. For reproducibility, at least six samples were measured for each gel and the results were averaged. The stress was presented by its nominal σ_{nom} or true values $\sigma_{\text{true}} (= \lambda\sigma_{\text{nom}})$, which are the forces per cross-sectional area of the undeformed and deformed gel specimen respectively, while the strain is given by λ , the deformation ratio (deformed length/initial length). The fracture stress σ_f and the % deformation at break were recorded. The Young's modulus E was calculated from the slope of stress–strain curves between deformation of 5% and 15%.

Since the gel samples both after preparation and in equilibrium with water did not break even at a strain of about 100% compression, the nominal stress σ_{nom} increased continuously with increasing strain. However, the corresponding $\sigma_{\text{true}}-\lambda$ plots pass through maxima indicating the onset of failure in the gel specimen. This behavior is likely a result of the self-healing ability of the hydrogels. Therefore, the fracture nominal stress σ_f and stretch λ_f at failure were calculated from the maxima in $\sigma_{\text{true}}-\lambda$ plots.

Self-Healing Behavior

To quantify the healing efficiency, tensile testing experiments were performed using virgin and healed cylindrical gel samples. Each experiment was carried out starting from a virgin gel sample. The virgin gel samples after synthesis and in equilibrium with water were cut in the middle, and then the two halves were merged together. For the hydrogels after preparation, in addition to autonomous healing at 23°C, temperature-induced healing tests were carried out at 80°C. The hydrogels formed using

CTAB in equilibrium with water were also subjected to healing tests under various healing conditions. The effects of the healing time and healing temperature as well as the treatment of the cut surfaces with acid or surfactant solutions were investigated. For this purpose, the gel samples were cut in the middle, and the cut regions were immersed (5 mm deep) into acidic solutions of CTAB and NaBr for 30 min at 35°C. Then, the two halves were merged together as described above. After repairing, the healed gel samples were transferred into water to remove surfactant and salts of the healing agent.

Rheological Experiments

Gelation reactions were carried out at 50°C within the rheometer (Gemini 150 Rheometer system, Bohlin Instruments). An angular frequency ω of 6.3 rad.s⁻¹ and a deformation amplitude γ_0 of 0.01 were selected to ensure that the oscillatory deformation is within the linear regime. After a reaction time of 1h, the dynamic moduli of the reaction solutions approached limiting values. Then, frequency-sweep tests were carried out at 25°C, as described before.^[14]

Results and Discussion

As described above, we prepared PAAC hydrogels with two types of surfactants by the micellar copolymerization of AAc with 2 mol.% C18. Figure 2 shows the swelling curves, photographs of such hydrogels in equilibrium in water and schematically depicts surfactant effect on hydrogels in water. Since pH inside the gels is equal to 1.5 at the state of preparation, PAAC is mostly protonated so that no complex forms between PAAC and surfactants. However, upon immersion of the gel samples in water, pH increases to 6.7, leading to the ionization of AAc units. This reveals that the gels formed in SDS solution exhibited a large swelling ratio ($m_{\text{rel}}=500\pm 70$) in water because of the osmotic pressure of AAc counterions and

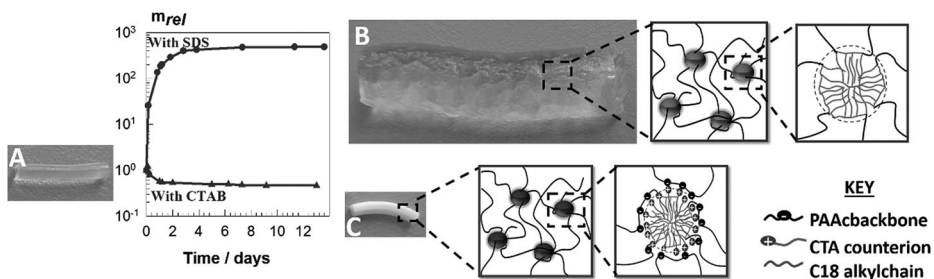


Figure 2.

Photographs of PAAc hydrogels (A) after preparation, (B) formed using SDS instead of CTAB significantly swell in water and (C) using CTAB deswell in water with reduction in the gel mass indicating the onset of complexation between PAAc and CTAB.

SDS progressively extracted from the network, the hydrophobic associations were so strong that they are not destroyed during the expansion of the gel network in water (Figure 2B).

As you seen in Figure 2C, a completely different swelling behavior is observed for PAAc hydrogels formed in solutions of oppositely charged cationic surfactant (CTAB). Hydrogels deswell in water with 60% reduction in the gel mass ($m_{rel}=0.37 \pm 0.2$) after gels were immersed in a large excess of water because PAAc is a polyelectrolyte whose repeating units bear an electrolyte group and forms a complex with cationic surfactants.^[16–18] Here, the surfactant alkyl chains are trapped electrostatically in a supramolecular polymer network formed via hydrophobic interactions. 70% CTAB bound to PAAc network

chains was calculated from the nitrogen contents of the dried gels, which were subjected elemental analysis measurements using a Thermo Flash EA-1112 Series elemental analyzer. The formation of PAAc-CTA complex is also obvious from the inspection of the gel samples. The hydrogels that are transparent after preparation became opaque in water.

Figure 3 represents stress–strain data of the physical gels after preparation (dashed lines) and in equilibrium with water (solid lines), as the dependence of the nominal stress σ_{nom} on % deformation. The characteristic tensile and compression data of the gels, i.e., the Young's modulus E , the fracture stress σ_f , and % deformation at break, are collected in Table 1. A significant enhancement in the mechanical properties of gels with CTAB is observable

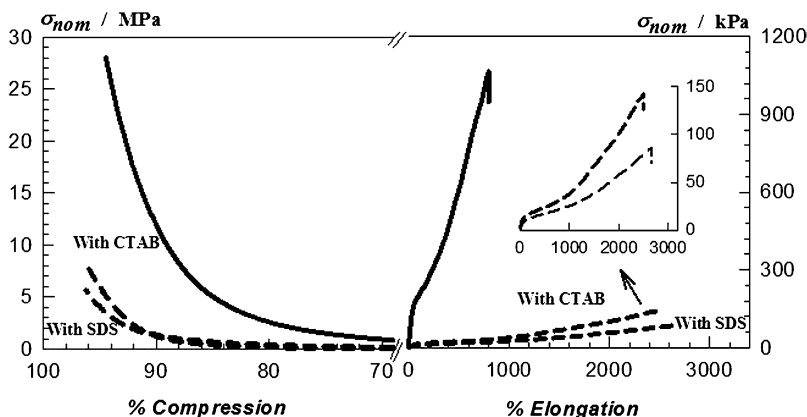


Figure 3.

Stress–strain curves of physical gels after preparation (dashes lines) and in equilibrium with water (solid lines).

Table 1.

Mechanical properties of PAAC hydrogels at the state of preparation and in equilibrium with water (E = Young's modulus and σ_f = fracture stress. Standard deviations are given in the parentheses).

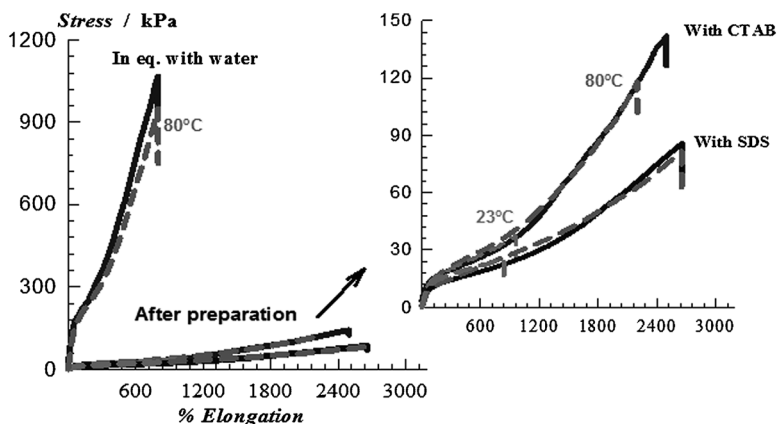
	Surfactant	After preparation			In water		
		E [kPa]	σ_f [MPa]	% at break	E [kPa]	σ_f [MPa]	% at break
Elongation	SDS	18 (2)	0.123 (0.005)	2890 (370)	*	*	*
	CTAB	16 (3)	0.150 (0.030)	2552 (120)	307 (42)	1.05 (0.14)	794 (62)
Compression	SDS	30 (3)	6.1 (0.4)	97 (1)	*	*	*
	CTAB	27 (4)	8.2 (0.6)	96 (2)	594 (113)	27 (2)	94 (1)

upon their immersion in water. 20-fold increase in the modulus E and 7-fold increase in the fracture stress σ_f were observed. Such a drastic change in the mechanical properties of gels upon their immersion in water is attributed to the extraction of CTA counterions from the micelles by AAC anions and simultaneous formation of ionic bonds at neutral pH. On the other hand, physical gels with SDS in water became weak and brittle to mechanical measurements because of the high equilibrium swelling ratios and extraction of SDS from the network.

To quantify the healing efficiency, tensile testing experiments were performed using virgin and healed cylindrical gel samples. In Figure 4, stress–strain curves of the virgin and healed gel samples formed at the state of their preparations are shown for a healing time of 30 min and for two different healing temperatures.

PAAC hydrogels at the preparation state, autonomic self-healing was observed within a time period of a few minutes. At 25°C, a complete recovery of the initial modulus E was observed while the healing efficiency with respect to the fracture stress. Healing efficiency increases with increasing temperature during healing due to the simultaneous increase of the chain mobility so that the polymer chains on the two cut surfaces can easily diffuse from one side to the other and the hydrophobes across the rupture interface become more accessible to each other.

PAAC hydrogels with CTAB after equilibrium in water were also subjected to healing tests. Although autonomic self-healing was not observed, increasing the healing temperature to 80°C induced healing within 30 min. As seen in Figure 4, after treatment of the cut surfaces with acid or surfactant solutions before heating to 80°C

**Figure 4.**

Stress–strain curves of the virgin (solid curves) and healed gel samples (dashed curves). Healing temperatures are indicated.

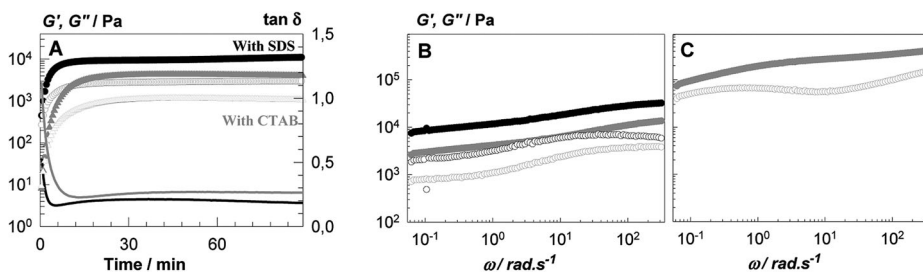


Figure 5.

(A) Elastic modulus G' (filled symbols), the viscous modulus G'' (open symbols), and loss factor $\tan \delta$ (lines) during the micellar copolymerization of AAC with 2 mol.% C18 at 50 °C shown as a function of the reaction time. (B) Frequency dependence of G' (filled symbols) and G'' (open symbols) for gels just after their preparation and (C) gels with CTAB after equilibrium with water.

further increased the healing efficiency and almost complete healing was achieved.

However, when swollen in water, such hydrogels with SDS formed by hydrophobic associations behave similarly to chemically cross-linked ones with time-independent elastic moduli, a high degree of spatial inhomogeneity, and no self-healing ability upon damage without any healing agent.^[14] It was shown that the drastic structural change in the physical gels upon swelling in water is due to the extraction of SDS micelles from the gel network, leading to the loss of the reversible nature of the cross-linkages. Thus, although mechanically weak and brittle gels could be obtained after removal of surfactant, the resulting gels lost their ability to self-heal, became too weak in the equilibrium swollen state in water and disintegrated into small gel particles during mechanical tests. This also prevents the application of self-healing hydrogels formed via hydrophobic interactions in aqueous environment.

A typical gelation profile of the micellar copolymerization reactions is shown in Figure 5A, where the elastic modulus G' , the viscous modulus G'' , and the loss factors $\tan \delta$ ($= G''/G'$) of the reaction system are plotted against the reaction time. The general trend is a rapid increase of the dynamic moduli followed by a plateau regime after a reaction time of about 1 h where the moduli slightly increase.

Figure 5B,C shows the frequency dependencies of G' (filled symbols) and G''

(open symbols) for the gels before and after swelling. The dynamic moduli of the physical gels are frequency dependent over the range of frequency between 0.08 and 400 rad s^{-1} , indicating their elastic and viscous energy dissipating properties. The dynamic moduli of the hydrogel increase by 1 order of magnitude upon immersion in water, suggesting the effect of complex formation between PAAc with CTA counterions. Further, both moduli of the gel are still frequency dependent and $\tan \delta$ remains above 0.1 after equilibrium in water, i.e., after extraction of free CTAB micelles. This behavior emphasizes viscous character of PAAc hydrogels in water environment, which is in strong contrast to the hydrogels forming no complex with SDS.

Conclusion

The physical gels with both SDS and CTAB showed similar properties after preparation, such as insoluble in water, exhibit time-dependent dynamic moduli, high fracture stress, high elongation ratios at break and high self-healing efficiency. Surfactant effect on such gels was seen when upon immersion in water and after extraction of free surfactant micelles. Physical gels with SDS were stable, exhibited high equilibrium swelling ratios and SDS progressively extracted from the network. The hydrophobic associations were so strong that they are not destroyed

during the expansion of the gel network in water. In contrast, the gel sample with CTAB in water exhibited very different behavior compared to with SDS. Hydrogels formed a complex and resulted in shrinkage after immersion in a large excess of water. PAAc-CTAB complexes exhibited unusual properties, such as high mechanical strength (up to 1.05 MPa tensile stress) and almost complete self-healing ability.

- [1] V. Amendola, M. Meneghetti, *Nanoscale* **2009**, 1, 74.
- [2] J. Cui, A. del Campo, *Chem. Commun.* **2012**, 48, 9302.
- [3] H. Zhang, H. Xia, Y. Zhao, *ACS Macro Lett.* **2012**, 1, 1233.
- [4] Q. Wang, J. L. Mynar, M. Yoshida, E. Lee, M. Lee, K. Okura, K. Kinbara, T. Aida, *Nature* **2010**, 463, 339.
- [5] J.-Y. Sun, X. Zhao, W. R. K. Illeperuma, O. Chaudhuri, K. H. Oh, D. J. Money, J. J. Vlassak, Z. Suo, *Nature* **2012**, 489, 133.
- [6] E. A. Appel, F. Biedermann, U. Rauwald, S. T. Jones, J. M. Zayed, O. A. Scherman, *J. Am. Chem. Soc.* **2010**, 132, 14251.
- [7] N. Holten-Andersen, M. J. Harrington, H. Birkedal, B. P. Lee, P. B. Messersmith, K. Y. C. Lee, J. H. Waite, *Proc. Natl. Acad. Sci. USA* **2011**, 108, 2651.
- [8] Y. Xu, Q. Wu, Y. Sun, H. Bai, G. Shi, *ACS Nano* **2010**, 4, 7358.
- [9] F. Liu, F. Li, G. Deng, Y. Chen, B. Zhang, J. Zhang, C.-Y. Liu, *Macromolecules* **2012**, 45, 1636.
- [10] G. Deng, C. Tang, F. Li, H. Jiang, Y. Chen, *Macromolecules* **2010**, 43, 1191.
- [11] P. Froimowicz, D. Klinger, K. Landfester, *Chem. Eur. J.* **2011**, 17, 12465.
- [12] S. B. Quint, C. Pacholski, *Soft Matter* **2011**, 7, 3735.
- [13] D. C. Tuncaboylu, M. Sari, W. Oppermann, O. Okay, *Macromolecules* **2011**, 44, 4997.
- [14] D. C. Tuncaboylu, M. Sahin, A. Argun, W. Oppermann, O. Okay, *Macromolecules* **2012**, 45, 1991.
- [15] U. Gulyuz, O. Okay, *Soft Matter* **2013**, 9, 10287.
- [16] U. Gulyuz, O. Okay, *Macromolecules* **2014**, 47, 6889.
- [17] P. F. C. Lim, L. Y. Chee, S. B. Chen, B.-H. Chen, *J. Phys. Chem. B* **2003**, 107, 6491.
- [18] J. Fundin, P. Hansson, W. Brown, I. Lidégran, *Macromolecules* **1997**, 30, 1118.